LGS WFS on ELTs II:Impact if the sodium layer fluctuations

Sandrine J. Thomas[1a], Nicolas Muller[23], Vincent Michau[2], and Thierry Fusco[2]

[1] UCO/Lick Observatory UCSC 1156 High Street, Santa cruz 95060, CA, USA
[2] Onera - The French Aerospace Lab, F-92322, Châtillon,, France
[3] Groupement d'intérêt Scientifique PHASE (Partenariat Haute résolution Angulaire Sol Espace) between Onera, Observatoire de Paris and Université Paris Diderot

Abstract. The application of laser guide stars to large aperture telescopes has spurred many new studies in wavefront sensing. For the particular case of the Shack-Hartmann WFS, wavefront sensing is prone to new sources of errors not previously considered. The primary source of error is spot elongation resulting from the resolution of the finite thickness of the sodium layer. The elongation spreads the signal over several pixels, resulting in a decrease of the signal to noise ratio and an increase of non-linearity. Also, the SHWFS performance becomes sensitive to temporal and spatial variations of the density of the sodium atoms. Among the different centroid algorithms to be used with this WFS, the most powerful methods (correlation, matched filter, WCoG) require a reference. Although straightforward for a point source, the use of a resolved laser guide star is more cumbersome because the sodium layer variations affect their performance. In this paper we look at the impact of the sodium layer fluctuations and the reference choice on the performance of the WFS, considering real as well as analytical non-symmetric profiles, and investigating both the subaperture level and the wavefront reconstruction level. We conclude on the compromise between the use of the best possible reference versus the difficulty of implementation.

1 Introduction

After being successfully used on 4 to 10m class telescopes such as the Lick, VLT, Gemini, Keck or others [1], [2], [3], laser guide stars (LGS) [4] are now part of most designs of future adaptive optics systems such as TMT and E-ELT. However, their implementation on larger telescopes is more challenging as one must account for errors which have been previously considered to be negligible – with natural guide stars or smaller telescopes. LGSs depend on the abundance and distribution of sodium atoms in the mesosphere and as a result present a unique set of difficulties. Moreover, the distribution of sodium atoms changes with time creating a variation in the average altitude of the layer. Viewed from the outer edge subapertures of a Shack-Hartmann Wavefront Sensor (SHWFS), the LGS appears strongly elongated. Because photons are spread over more pixels, the signal-to-noise ratio (SNR) decreases for a given laser power. Furthermore, due to the elongation, the variations of the sodium atoms distribution will be resolved at the outer edges, leading to erroneous wavefront measurements, primarily defocus. The SNR obtained for the LGS image directly affects the accuracy of the wavefront measurement obtained from the SHWFS. When the effects of elongation and variability of the sodium layer on SNR are considered, the potential impact on performance is significant. The variability in altitude and thickness of the sodium layer can also lead to errors in focus or even truncation of the LGS image, contributing to additional sources of degradation in wavefront measurement accuracy.

Many groups are studying these problems using different approaches. Lardiere et al. [5] use a testbed to simulate the elongation of the spot on a SHWFS and study the performance of different algorithms considered in the context of the TMT [6]. More theoretical studies [7], [8], [9] describe the expected errors analytically. Using Equation (1) from the first part of this study (LGS WFS on ELTs I) [10], the error made using a Shack-Hartmann wavefront sensor is written as:

$$E = E_{noise} + E_{NL,turb} + E_{NL,Na}, \tag{1}$$

where E_{noise} is the measurement noise, $E_{NL,turb}$ is the error coming from the interaction between the non-linearities and the turbulent propagation and $E_{NL,Na}$ is the non-linearity error due to the spatial and

[a] sthomas@gemini.edu

temporal variations of the sodium layer. In the first part of this study, the authors [10] present the effect of non-linearity due to sampling and truncation ($E_{NL,turb}$) relative to the noise. In this paper, we are presenting the effect of the sodium profile variations ($E_{NL,Na}$) both on the spatial structure and in time also relative to the noise. These effects are seen when using specific algorithms, namely correlation [11], matched filter [12] and weighted center of gravity [13]. For sake of clarity we are focussing on the correlation method, which gave us the best performance in previous study (and similar to matched filtering). Along with studying the effects of asymmetric profiles and their evolution over time, we studied the optimum choice of reference for correlation algorithm. The answer will give clues on the best implementation for the wavefront measurement in presence of an LGS. Knowing the impact of the fluctuation of the sodium density in the sodium layer is important in order to define the correct reference for the correlation calculation. The fluctuations are insignificant for smaller telescopes as the elongated spot is not resolved. However, when using larger telescopes, these variations will be resolved and will affect the centroid calculation. Also, the spot motion will be due to both the atmospheric turbulence and the sodium layer fluctuations. The latter introduces non-common path errors since the wavefront measurement results from the LGS and not the science target.

The first section presents a summary of the real profiles gathered at Lick Observatory [14]. The second shows the impact of sodium layer variations on the wavefront sensor measurements at the subaperture level. In section three, we show the results at the wavefront reconstruction level in the context of the Thirty Meter Telescope (TMT). During this study, we looked at the difference between using a polar coordinate CCD [15] and a regular cartesian CCD.

2 Real data from the Lick Observatory

In order to understand the real impact of the sodium layer on the centroid measurements and thus on the wavefront reconstruction, it is necessary to include real data in the simulations. Several groups have looked into such experiments using real lasers [16], LIDAR data [17] or existing LGS AO systems. We used a 1 m telescope at the Lick Observatory to observe a laser launched from the adjacent 3 m telescope, located 600 m away. We gathered a total of 6 nights of data presented in Thomas et al. [14]. The temporal resolution is of the order of 1 s and the spatial resolution of the order of 75 m. These resolutions are sufficient to observe the impact of the structural evolution on the measurement since the final WFS subaperture images are re-sampled to coarser resolution. On average, the spatial resolution drops from 75m on sky to about 1.5km on the SHWFS detector for Nyquist sampling and a seeing if 1.19 arcsec.

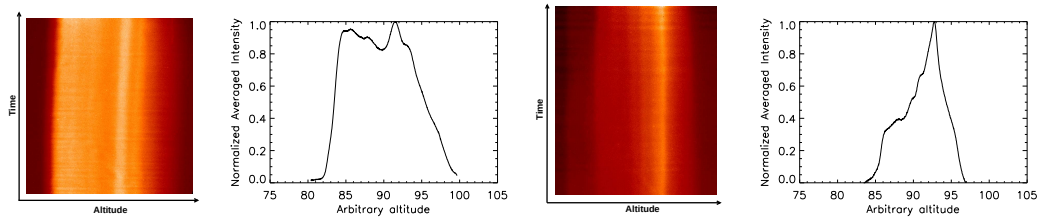

Fig. 1. Example of the profiles observed on October 10th, 2006. The left set of data was taken at 1:18 am and the right one at 4:56 am. The variation in shape is obvious.

For this paper, we focus on the nights of September 9th 2006 and October 10th, 2006 because of their many image profiles and good range of shapes (see Thomas et al [14] for more details). When looking at the turbulence evolution on the two-dimensional images for October 10th 2006, the distribution changes on a large temporal scale. The distribution is broad at the beginning, resembling a top-hat function, whereas at the end of the night the shape becomes more Gaussian with a distinct central peak. The two extreme cases are shown in figure 1. The average images are calculated from the drift scan image, taken over approximatively 300s.

To complement the study described in [14], we classified the profiles using moments. Indeed, each profile can be characterized by a set of moments, the n^th moment μ_n being defined with regards to the central moment $\mu_n = \langle (x - \langle x \rangle)^n \rangle$. We focused on the first four – mean, variance, skewness and kurtosis – as they define the main shape of the profile to the level of resolution we have on a outer-edge subaperture. This might vary with the size of the telescope. Looking at the whole set of data from Lick Observatory, we extracted a trend for each moment, allowing us to simplify the reference used in the calculation of the centroid. The variation of the first four moments as a function of profile is shown on Figure 2. The first moment is constant after removal of the mean (moment 1, on Figure 2, top left). The other moments vary and allow us to isolate a few interesting cases.

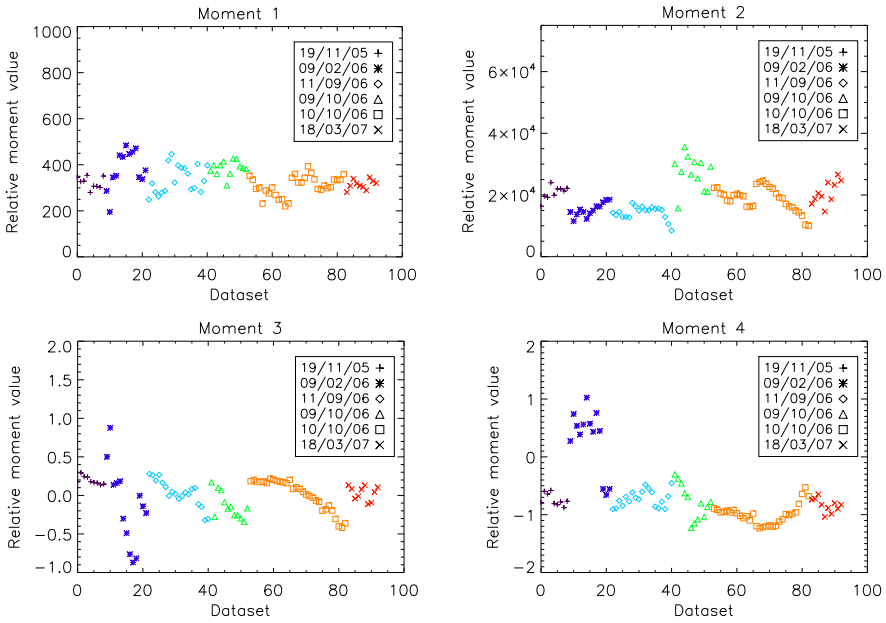

Fig. 2. First four moments for the set of data obtained at Lick Observatory. From top left to bottom right, we show the mean (M1), variance (M2), skewness (M3) and kurtosis (M4). Each symbol represents a different night.

Muller et al. [10] are using those values to create their analytical profiles. For this site and during fall to spring, meaningful values are in the range of [-0.5-0.5] for M3 and [-1,1] for M4. Using these profiles we looked at the impact of the sodium layer both at the subaperture level and the phase reconstruction level.

3 Error due to fluctuations in the sodium profile in the context of the TMT

The correlation algorithm needs a reference to correlate the signal with. In the case of a small telescope the reference is usually a Gaussian spot. However, a better reference is needed when using larger telescopes, especially when side launch is considered. For this proceeding, the telescope considered is the TMT and the laser guide star is launched from the center of the mirror. This decreases the elongation to 15m versus the 42m for the case of the E-ELT [10]. This latter case will be studied in a future paper. The references considered are listed below, along with the notation used in the following of the paper. We also list the implementation repercussions of the different references.

– LGS Ref 1: *Ideal reference, copy of the image without noise.* This reference uses the exact profile and therefore requires external devices with better resolution to measure the instantaneous profile. The measurement has to also track the focus very accurately.

- LGS Ref 2: *Average of the images in the subaperture at the same distance with noise.* This reference does not require an external device, only software changes. A study of the time required for the calculation is needed. The simulation might be optimistic but gives a good idea at least in the configuration of the polar coordinates CCD.
- LGS Ref 3 and 4: *Temporal average of the previous frame respectively without and with noise.* Another reference option is to use an average over the previous images with or without noise. The sodium profile does not change significantly for a few seconds and the actual fast spot motion due to the atmospherical turbulence can be isolated. The impact will be mainly a change in focus, which is negligible in close loop. LGS Ref 3 is without noise, while LGS Ref 4 has noise. For these proceedings, we fixed the time during which we use the previous averages to 10 s, hence relatively fast. We are planning to vary this parameter in another paper. This method does not require an external instrument and in addition does not need to be as instantaneous as LGS Ref 2.
- LGS Ref 5 and 6: *Temporal average from a frame taken at the beginning of the night respectively without and with noise.* A more extreme version of the previous reference is to use data from the beginning of each night. This method is not optimal as the profile can vary significantly in shape and average altitude during the night. However, as for the previous method, the evolution is slower and will probably not limit the error budget. LGS Ref 5 is without noise, while LGS Ref 6 has noise. The average was done over a 10 s interval.
- LGS ref 7: *A profile generated from moments.* We used a synthetic profile made from one profile from the September data and applied it both to the October batch and the September batch. The advantage of this method is that we can reconstruct the profile from a site study. From the previous section, we can use typical values for M2-M4 to reconstruct the profile. The impact on the timing is null and we do not need any external instrument.
- LGS ref 8: *A Gaussian reference.* Finally, we used an even simpler version of LGS Ref 7 by limited the profile reconstruction to only M2, i.e. the standard deviation. In other word, we use a Gaussian as a reference and suppose that the barely resolved variations of the sodium layer are negligible compared to the overall elongation. This choice of reference, if comparable to all the other ones, would be the simplest to implement. The only knowledge required is the size of the spot.

Using all these different references, we looked at their impact on the wavefront sensor measurement error, both at a subaperture level and wavefront level.

The context chosen here is the TMT [18], whose parameters are shown in table 1 [19],[20]. A similar study for the E-ELT is presented by Muller et al [10]. For the TMT, the laser will be central-launched, reducing the elongation. Also, a new type of CCD, called the polar coordinate detector [15] is being developed with the objective of improving the performance. This CCD provides a rectangular imager for each subaperture of the SHWFS. The major axis of the imager is oriented to match the axis of perspective elongation for the LGS image. The number of pixels in each subaperture is optimized to match the size of the elongated LGS image therefore providing optimal sampling of the image, without truncation. It also allows fast reading. Table 1 shows the main parameters that we used.

Table 1. Parameters for TMT study relevant for this paper.

Parameter	Values
Number of photons	1000 photons
Readout noise	N_r 3 e^-
Sodium (Na) layer thickness	from 10 km to 20 km
Operating wavelength	589 nm
Spot size (non-elongated)	1.19”(typical seeing, no uplink correction)
Telescope diameter	30 m
Number of subapertures	60×60
Subaperture field of view	20 by 20 pixels
Sampling	1-3 pixels per FWHM

4 Results at the subaperture level

The first step is to study the effect of the reference at the subaperture level, with and without noise. The goal is to get an appreciation of when the elongation start be significant. We studied four different configurations, namely the TMT configuration using a polar CCD with and without noise as well as the cartesian configuration also with and without noise. We also looked at different profiles taken during different nights. Finally, we only show results for the correlation method for sake of conciseness.

Figure 3 shows the behaviour of the error as a function of the subaperture distance from the center of the pupil. Because the results are identical to within 1% between the cartesian and polar configurations, we only show the results of the cartesian CCD. We also only show results for September 19th 2006 and October 10th 2006. The moments for these nights are respectively the following: M2=15,M3=-1,M4=-0.5 and M2=22,M3=0,M4=-1 As expected, the lowest error is reached when the

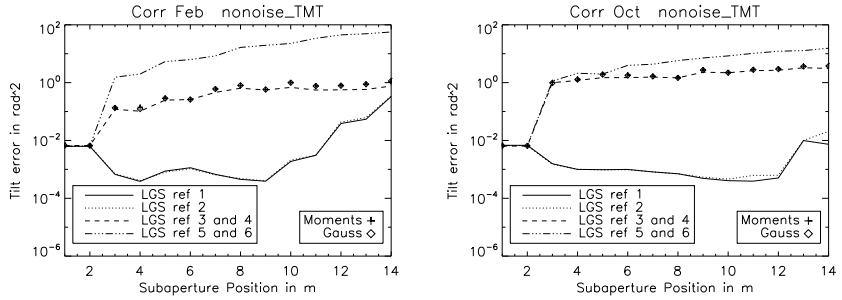

Fig. 3. Total tilt error in rad^2 (i.e. considering both axis) as a function of the subaperture position, for different references. The centroid method is the correlation and there is no noise. The left graph corresponds to a profile in February and the right graph from October.

reference is the exact profile without noise or when using an average of the profiles over identical subapertures. This also makes sense as we end up recreating the exact reference. The rest of results are gathered in two groups. The average over a few previous seconds (Ref 5), as well as the synthetic reference (Ref 7) and the Gaussian reference (Ref 8) give better results than an average reference taken at the beginning of the night. For this last statement, there is a slight difference between the two nights considered. The noise for the night in October is lower than the other night, which can be explained by the difference in shape evolution. These results are in agreement with those of Muller et al. [10].

Figure 4 shows the error with low level noise (500 photons and no readout noise) as well as with higher noise (500 photons and a readout noise of 3 electrons). For the night of February, the results are noise limited for most references except the one taken at the beginning of the night. For the night of October however, the system is noise limited only for the higher noise level. For the case of no readout noise, the choice of the reference does matter to a factor 2.5 between the best and the worst results. In any case, this first step shows that there is no need for an external telescope since we can use data from the Shack-Hartman itself to create the reference.

5 Results at the reconstructed wavefront level

The reconstruction itself is done using a Fourier Reconstruction [21]. We then projected the phase on the Zernike polynomials to check the main aberrations introduced by the fluctuations of the sodium layer. Also, compared to Muller et al. [10], we only use one laser guide star and reconstruct the wavefront on axis. This, added to the fact that we are using a smaller telescope, explains why the performance presented here are better than the ones presented in Muller et al. [10]. We run the simulations for the same configurations as the ones presented in the previous section, for both September and October. Figure 5 shows example of reconstructed wavefront

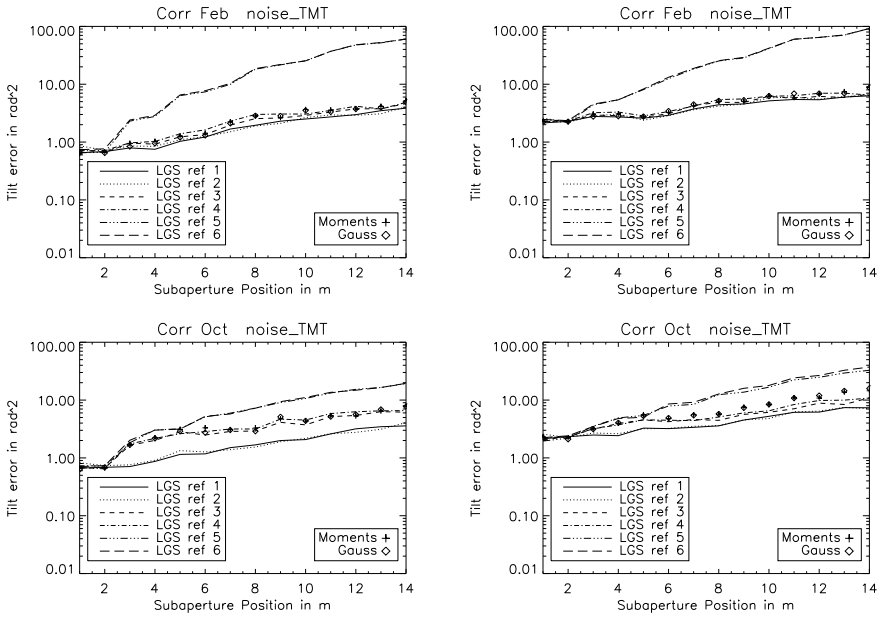

Fig. 4. Total tilt error in rad^2 as a function of the subaperture position, for different references. The centroid method is the correlation and we considered two levels of noise. The graph on the left corresponds a noise level of 500 photons and no readout noise and the graph on the right corresponds a noise level of 500 photons and a readout noise of 3 electrons. The top row shows results from February and the bottom on shows results from October.

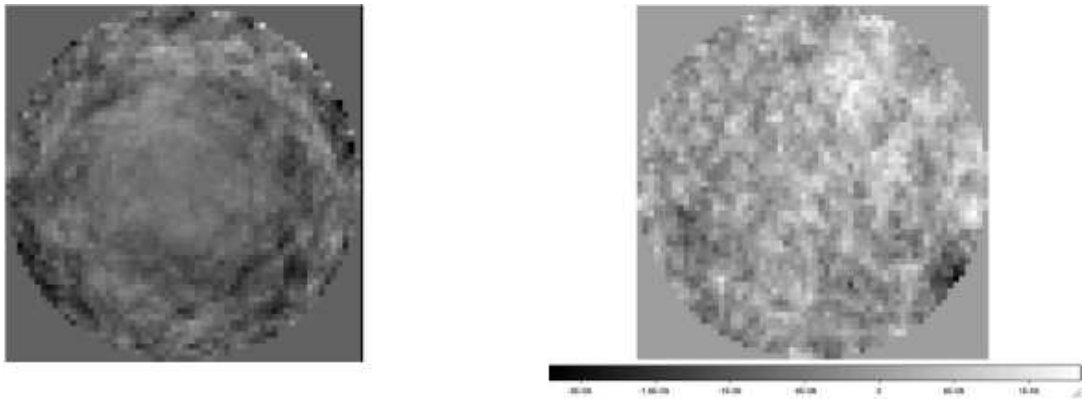

Fig. 5. Reconstructed wavefront without noise (left) and with noise (right). The graphs show results for the TMT configuration and with noise (we used 500 photons and a readout noise of 3 electrons).

Figure 6 shows the Zernike decomposition of the reconstructed wavefront as a function of the reference. The results are for the polar coordinate CCD although there is very little difference between using a polar and cartesian detector in our simulations. The noise level is high (500 photons and a readout noise of 3 electrons). Without noise, the results are very similar, only the value of the errors decreases.

The results are in agreement with those of the previous section. If the reference is the same as the profile or taken from an average of similar subapertures, the reconstructed wavefront has the lowest noise. If the reference is from profiles taken in within 10 seconds of the measurement, the error goes up

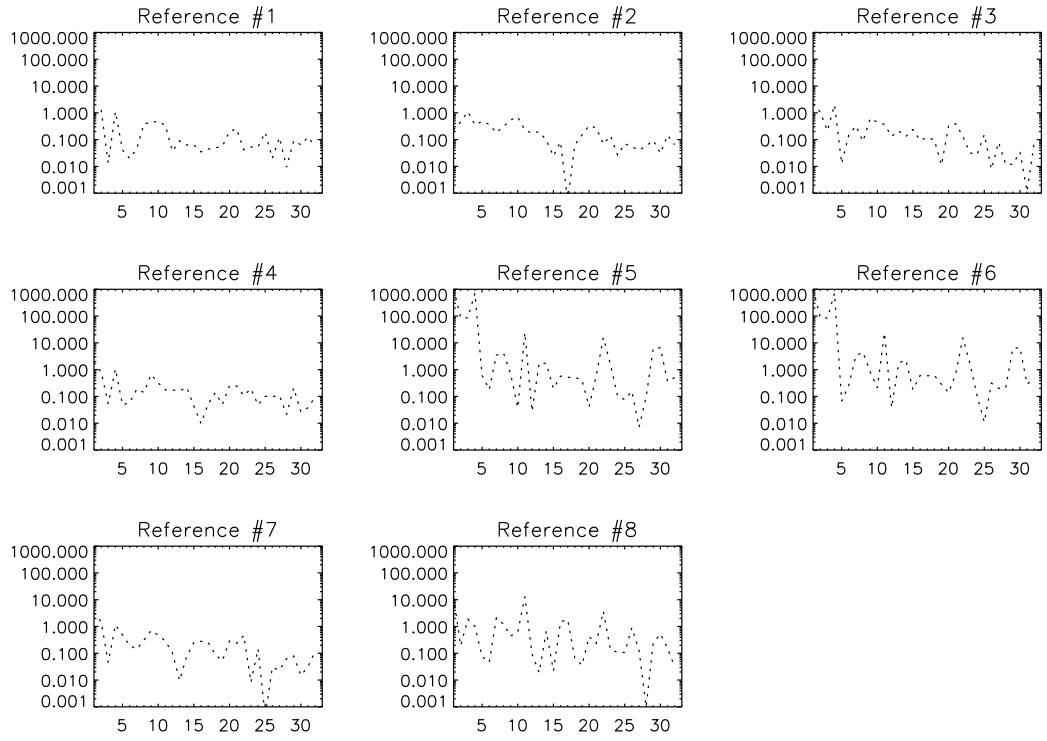

Fig. 6. Wavefront error as a function of Zernike coefficients for different reference. The number corresponds to the reference listed in 3. The graph shows results with the TMT configuration, 500 photons and a readout noise of 3 electrons.

but remains lower than a few nm rms. However, if the reference is from the beginning of the night the error goes up, especially in focus. This is expected since the main error will increase as a function of the subaperture position. Finally, using a profile reconstructed from moments, the error is comparable to the case LGS Ref 3/4.

We measured around 20nm rms for a profile with skewness of -1 and kurtosis of -0.5. This is of the same order of magnitude as Muller et al. [10]. They found errors of the order of 60nm rms, for a tomography reconstructed wavefront and a laser launch from the side of a 40m telescope. Assuming crudely that the error is linear, our configuration should give errors at least 2.5 times lower. One promising reference is the average over subapertures located at the same distance from the center (LGS 2). Conveniently, in the configuration where the LGS is launched from the center, the number or subapertures available for the average increases as a function of distance and thus elongation. The reference is therefore getting less noisy for outer edge subapertures. However, the results presented in this paper regarding this case might be biased since we did not take into account the rotation and pixelisation of the image when added up the frames. More precise work would need to be done to give a definitive answer. However, the graph shows again that using a profile reconstructed from typical moments (Ref 7) is as good as using an average of the previous frames.

6 Conclusions

In this paper we looked at the impact of the choice of the reference mainly for the correlation algorithm. We looked both at the subapeture level and the reconstructed wavefront. From this study we can conclude that in the context of the TMT, the error due to the reference is negligible compared to

readout and photon noise. There is no need for complicated method to measure the sodium profile accurately since using simpler references than the exact profile give similar errors to within 10nm rms. The resulting wavefront error due to reference error is less than 20nm rms in presence of noise and is in agreement with [10]. Moreover, the best overall options are either using the average over subapertures located at the same distance or using a profile reconstructed from typical moments. These results are mainly for two nights out of the six available to us. However, it gives a good understanding and provides insights to the problem. A future paper should verify that these results are consistent for all nights.

References

1. Bouchez, A. H., Mignant, D. L., van Dam, M. A., Chin, J., Hartman, S., Johansson, E., Lafon, R., Stomski, P., Summers, D., and Wizinowich, P. L. *Advancements in Adaptive Optics. Edited by Domenico B. Calia* **5490**, 321 (Oct 2004).
2. Bonaccini, D., Allaert, E., Araujo, C., Brunetto, E., Buzzoni, B., Comin, M., Cullum, M. J., Davies, R. I., Dichirico, C., Dierickx, P., Dimmler, M., Duchateau, M., Egedal, C., Hackenberg, W. K. P., Hippler, S., Kellner, S., van Kesteren, A., Koch, F., Neumann, U., Ott, T., Quattri, M., Quentin, J., Rabien, S., Tamai, R., Tapia, M., and Tarenghi, M. *Adaptive Optical System Technologies II. Edited by Wizinowich* **4839**, 381 (Feb 2003).
3. Gavel, D. T., Gates, E. L., Max, C. E., Olivier, S. S., Bauman, B. J., Pennington, D. M., Macintosh, B. A., Patience, J., Brown, C. G., Danforth, P. M., Hurd, R. L., Severson, S. A., and Lloyd, J. P. *Adaptive Optical System Technologies II. Edited by Wizinowich* **4839**, 354 (Feb 2003).
4. Foy, R. and Labeyrie, A. *Astronomy and Astrophysics (ISSN 0004-6361)* **152**, L29 (Nov 1985).
5. Lardiere, O., Conan, R., Bradley, C., Jackson, K., and Herriot, G. *Optics Express* **16**, 5527 (Apr 2008).
6. Conan, R., Lardière, O., Herriot, G., Bradley, C., and Jackson, K. *Applied Optics* **48**, 1198 (Feb 2009).
7. Thomas, S. J., Adkins, S., Gavel, D., Fusco, T., and Michau, V. *Monthly Notices of the Royal Astronomical Society* **387**, 173 (Jun 2008).
8. Michau, V., Conan, J.-M., Fusco, T., Nicolle, M., Robert, C., Velluet, M.-T., and Piganeau, E. *Atmospheric Optical Modeling* **6303**, 10 (Sep 2006).
9. Gratadour, D., Gendron, E., and Rousset, G. *Journal of the Optical Society of America A* **27**, 171 (Sep 2010).
10. Muller, N., Thomas, S., Michau, V., and Fusco, T. *This conference* (2012).
11. Poyneer, L. A. *Applied Optics* **42**, 5807 (Oct 2003).
12. Gilles, L. and Ellerbroek, B. *Applied Optics IP* **45**, 6568 (Sep 2006).
13. Nicolle, M., Fusco, T., Rousset, G., and Michau, V. *Optics Letters* **29**, 2743 (Dec 2004).
14. Thomas, S. J., Gavel, D., and Kibrick, R. *Applied Optics* **49**, 394–402 (Jan 2010).
15. Adkins, S. M., Azucena, O., and Nelson, J. E. *Advances in Adaptive Optics II. Edited by Ellerbroek* **6272**, 43 (Jul 2006).
16. d'Orgeville, C., Rigaut, F. J., Boccas, M., Dainty, C., Figueroa, E., Flicker, R., Gregory, B., Michaille, L., Quartel, J. C., Tokovinin, A. A., Trancho, G., and Wooder, N. J. *Adaptive Optical System Technologies II. Edited by Wizinowich* **4839**, 492 (Feb 2003).
17. Pfrommer, T., Hickson, P., and She, C.-Y. *Geophys. Res. Lett.* **36**, 15831 (Aug 2009).
18. Nelson, J. and Sanders, G. H. *Ground-based and Airborne Telescopes II. Edited by Stepp* **7012**, 44 (Aug 2008).
19. Ellerbroek, B., Britton, M., Dekany, R., Gavel, D., Herriot, G., Macintosh, B., and Stoesz, J. *Astronomical Adaptive Optics Systems and Applications II. Edited by Tyson* **5903**, 20 (Aug 2005).
20. Herriot, G., Hickson, P., Ellerboek, B. L., Andersen, D. A., Davidge, T., Erickson, D. A., Powell, I. P., Clare, R., Gilles, L., Boyer, C., Smith, M., Saddlemyer, L., and Véran, J.-P. *Advances in Adaptive Optics II. Edited by Ellerbroek* **6272**, 22 (Jul 2006).
21. Poyneer, L. A., Gavel, D. T., and Brase, J. M. *Journal of the Optical Society of America A* **19**, 2100 (Oct 2002).